Vibrational Spectroscopic Study of Thiophenolate-Capped Nanoclusters of CdS and of Cadmium Thiophenolate Complexes

Thomas Løver, Graham A. Bowmaker,* John M. Seakins, and Ralph P. Cooney

Department of Chemistry, University of Auckland, Private Bag 92019, Auckland, New Zealand

Received October 14, 1996. Revised Manuscript Received January 30, 1997[⊗]

Thiophenolate-capped nanoclusters of cadmium sulfide and the cadmium thiophenolate compounds $Cd(SPh)_2$, $[Cd(SPh)_4](Me_4N)_2$, $[Cd_4(SPh)_{10}](Me_4N)_2$, and $[Cd_4X_4(SPh)_6](Et_4N)_2$ (X = Cl, Br, I) have been studied by low-frequency FT-IR and Raman spectroscopy. In the spectrum of the cluster $[S_4Cd_{10}(SPh)_{16}](Me_4N)_4$ a band at 288 cm^{-1} was assigned to the ν(Cd−S) stretching modes of the (Cd−S) bonds of the S_4Cd_6 cluster core. The ν(Cd−S) stretching frequencies of the bridging and terminal SPh^- ligands which cap the cluster core were assigned to bands in the region 150−187 cm^{-1}. The ν(Cd−S) core band for $[S_4Cd_{17}(SPh)_{28}](Me_4N)_2$ with tetracoordinated sulfides, as in bulk CdS, was observed at 270 cm^{-1}. The far-infrared ν(Cd−S) core band showed a progressive broadening and shift from 270 cm^{-1} toward the peak position of 241 cm^{-1} in bulk (wurtzite) CdS with increasing cluster size up to ca. 40 Å. This shift is interpreted in terms of an increase in the average Cd−S bond length. Far-infrared spectroscopy has been shown to be a valuable technique for the characterization of thiolate-capped metal chalcogenide clusters.

Introduction

Nanometer-sized semiconductor clusters are a class of materials of considerable current interest. In this intermediate size regime (10−60 Å, 15−4000 atoms for CdS) a gradual transition from solid-state to molecular structure occurs as the particle size decreases. A splitting of the energy bands into discrete, quantized levels occurs. The optical, electronic, and catalytic properties of such nanoparticles (quantum dots) differ markedly from the corresponding macrocrystalline substance,[1−6] and studies have shown a strong size and dimensionality dependence of these properties.[7] With the development of methods that permit uniform clusters to be prepared, a new trend of research is evolving with the aim of arranging individual particles in two- and three-dimensional superlattices and investigating the collective properties resulting from the interactions of the particles.[8] One method that has produced highly monodisperse samples involves the use of ligands that cap the particle surface by direct coordination to surface atoms. This has proved effective for clusters of metal chalcogenides (ME; M = Cd, Zn; E = S, Se) using mainly thiolates and in particular thiophenolate (SPh^-) as the capping ligand.[9−19] The process involves precipitation of the semiconductor material in the presence of the capping species, or growth of larger clusters from molecular precursors which already incorporate the capping ligands. Steigerwald et al.[16] discovered that micelle-encapsulated CdS particles capped with SPh^- ions could be grown in a controlled manner by additions of S^{2-} ions to the microemulsion. The particles increased in size by an inorganic polymer-like process where added sulfide displaces the caps and builds up a new CdS layer, followed by the reattachment of caps to the particle surface. Following this, Herron et al.[17] mixed a solution of Cd^{2+} ions with a solution containing a mixture of $S^{2-}$and SPh^-. Adjustment of the sulfide-to-thiophenolate ratio caused the competitive reaction rates of these species with Cd^{2+} ions to control the eventual cluster size. The clusters reported ranged in size from <15 to 35 Å. Addition of S^{2-} ions to a solution of $[S_4Cd_{10}(SPh)_{16}](Me_4N)_4$ has been shown to result in the growth of a ca. 10 Å cluster with the proposed formula $[S_{13}Cd_{20}(SPh)_{22}](Me_4N)_8$.[18] More recently the 15 Å clusters $[S_{14}Cd_{32}(SPh)_{36}]\cdot 4(DMF)$ and $[S_{14}Cd_{32}(SCH_2CH(OH)CH_3)_{36}]\cdot 4H_2O$ have been crystallized and fully characterized.[19,13] Other well-defined SPh^- capped clusters which have been isolated as crystalline solids

[⊗] Abstract published in *Advance ACS Abstracts,* March 15, 1997.

(1) Brus, L. E. *Appl. Phys. A* **1991**, *53*, 465.
(2) Wang, Y.; Herron, N. *J. Phys. Chem*. **1991**, *95*, 525.
(3) Bawendi, M. G.; Steigerwald, M. L.; Brus, L. E. *Annu. Rev. Phys. Chem*. **1990**, *41*, 477.
(4) Hengelein, A. *Top. Curr. Chem*. **1988**, *143*, 113.
(5) Hengelein, *A. Chem. Rev*. **1989**, *89*, 1861.
(6) Wang, Y.; Herron, N. *Phys. Rev. B* **1990**, *42*, 7253.
(7) Weller, H. *Angew. Chem., Int. Ed. Engl.* **1993**, *32*, 41.
(8) Weller, H. *Angew. Chem., Int. Ed. Engl.* **1996**, *35*, 1079.
(9) Murray, C. B.; Norris, D. J.; Bawendi, M. G. *J. Am. Chem. Soc.* **1993**, *115*, 8706.
(10) Noglik, H.; Pietro, W. *J. Chem. Mater*. **1994**, *6*, 1593.
(11) Nosaka, Y.; Shigeno, H.; Ikeuchi, T. *J. Phys. Chem*. **1995**, *99*, 8317.
(12) Hayes, D.; Micic, O. I.; Nenadovic, M. T.; Swayambunathan V.; Meisel, D. *J. Phys. Chem*. **1989**, *93*, 4603.
(13) Vossmeyer, T.; Reck, G.; Schulz, B.; Katsikas, L.; Weller, H. *J. Am. Chem. Soc.* **1995**, *117*, 12881.
(14) Marcus, M. A.; Flood, W.; Stiegerwald, M.; Brus L.; Bawendi, M. *J. Phys. Chem*. **1991**, *95*, 1572.
(15) Kortan, A. R.; Hull, R.; Opila, R. L.; Bawendi, M. G.; Steigerwald, M. L.; Carrol, P. J.; Brus, L. E. *J. Am. Chem. Soc.* **1990**, *112*, 1327.
(16) Steigerwald, M. L.; Alivisatos, A. P.; Gibson, J. M.; Harris, T. D.; Kortan, R.; Muller, A. J.; Thayer, A. M.; Duncan, T. M.; Douglass, D. C.; Brus, L. E. *J. Am. Chem. Soc.* **1988**, *110*, 3046.
(17) Herron, N.; Wang, Y.; Eckert, H. *J. Am. Chem. Soc*. **1990**, *112*, 1322.
(18) Herron, N.; Suna A.; Wang, Y. *J. Chem. Soc., Dalton Trans*. **1992**, 2329.
(19) Herron, N.; Calabrese, J. C.; Farneth, W. E.; Wang, Y. *Science* **1993**, *259*, 1426.

S0897-4756(96)00534-0 CCC: $14.00

are $[ECd_8(SPh)_{16}](Me_4N)_2$,[20] $[E_4M_{10}(SPh)_{16}](Me_4N)_4$ (M = Cd, Zn; E = S, Se, Te),[21] $[S_4Cd_{17}(SPh)_{28}](Me_4N)_2$,[22] and $[S_4Cd_{17}(SCH_2CH_2OH)_{26}]$.[23] However, in general, crystallization of these materials is difficult, resulting in less rigorous characterization of chemical structure and particle dimensions by methods such as X-ray powder diffraction, UV−visible spectroscopy, and transmission electron microscopy (TEM). Recently the existence of $[SCd_4(SEt)_{12}]^{6-}$, $[SCd_8(SEt)_{16}]^{2-}$, $[S_4Cd_{10}(SEt)]_{12}$, and $[S_4Cd_{17}(SEt)_{24}]^{2+}$ in solution have been suggested on the basis of NMR studies.[24] Only very limited vibrational data have been reported.[25,26] The vibrational frequencies of the (Cd−S) bonds were expected to be sensitive to the structure type and the identity of the sulfur atoms. Low-frequency (50−500 cm^{-1}) vibrational spectroscopy should therefore be of value in the characterization of the core and surface structures and for monitoring changes in bonding accompanying structural changes during growth of nanoclusters from molecular precursors. We present the vibrational spectra of several cadmium thiophenolate complexes with structures that are similar to that of the capping layer of the clusters. These form the basis for the analysis of the spectra of clusters of CdS, CdSe, ZnS, and ZnSe (with an emphasis on CdS) in the size range 7−40 Å.

Experimental Section

Spectroscopy. FT-IR spectra were obtained at 4 cm^{-1} resolution with a Digilab FTS-60 spectrometer employing an FTS-60V vacuum optical bench with a mercury lamp infrared source, a 6.25 μm Mylar film beam splitter, and a pyroelectric triglycine sulfate (TGS) detector. Samples were dried under vacuum and then pressed into disks in powdered polyethylene. Raman spectra were obtained using a JY U1000 Raman spectrometer with a green 514 nm argon laser set to give 30 mW on the sample. UV spectra of cluster materials dissolved in acetonitrile were obtained with a Shimadzu Model UV-2101PC using a 10 mm path length quartz cell. Thermal analysis measurements were recorded using a Polymer Laboratories PL-DSC 12000 differential scanning calorimeter and a PL-STA 1000/1500 simultaneous thermal analyzer with a ramp rate of 10 °C/min.

Materials Preparation. *Cadmium Thiophenolate Complexes.* The compounds $[Cd(SPh)_4](Me_4N)_2$ and $[Cd_4(SPh)_{10}](Me_4N)_2$ were prepared from stoichiometric amounts of thiophenol (PhSH), triethylamine (Et_3N), cadmium nitrate ($Cd(NO_3)_2$), and tetramethylammonium chloride ([Me_4N]Cl) in acetonitrile by the previously described method.[21] The three compounds $[Cd_4X_4(SPh)_6](Et_4N)_2$ (X = Cl, Br, I) were prepared by addition of benzoyl chloride (PhCOCl), bromine (Br_2), and iodine (I_2) to a solution of $[Cd_4(SPh)_{10}](Et_4N)_2$ in acetone following the method described by Dean.[27] Found for $[Cd_4Cl_4(SPh)_6](Et_4N)_2$: C 41.99, H 4.43, N 1.64%. Calculated: C 41.45, H 4.68, N 1.86%. Found for $[Cd_4I_4(SPh)_6](Et_4N)_2$: C 34.02, H 3,73, N 1.38%. Calculated: C 33.35, H 3.77, N 1.50%. The compound $Cd(SPh)_2$ was prepared by standard methods from stoichiometric amounts of HSPh, Et_3N, and $Cd(NO_3)_2$ in methanol.[28]

Clusters. *$[E_4M_{10}(SPh)_{16}](Me_4N)_4$ (M = Cd, Zn; E = S, Se).* The clusters $[S_4Cd_{10}(SPh)_{16}](Me_4N)_4$, $[Se_4Cd_{10}(SPh)_{16}](Me_4N)_4$, $[S_4Zn_{10}(SPh)_{16}](Me_4N)_4$, and $[Se_4Zn_{10}(SPh)_{16}](Me_4N)_4$ were prepared by additions of elemental sulfur or selenium to a solution of $[M_4(SPh)_{10}](Me_4N)_4$ (M = Cd, Zn) in acetonitrile as previously described.[21]

$[S_4Cd_{17}(SPh)_{28}](Me_4N)_2$. The CdS cluster $[S_4Cd_{17}(SPh)_{28}](Me_4N)_2$ was prepared in a self-assembly reaction of PhSH, Et_3N, $Cd(NO_3)_2$, Na_2S, and $(Me_4N)Cl$ in methanol/acetonitrile as described in the literature.[22,29]

The material contained chloride impurities and consisted of $[S_4Cd_{17}(SPh)_{28}](Me_4N)_2$, $[S_4Cd_{17}(SPh)_{27}Cl](Me_4N)_2$, and $[S_4Cd_{17}(SPh)_{26}Cl_2](Me_4N)_2$ in the ratio 100:31:3 as determined by electrospray mass spectroscopy (ESMS). Found: C 40.03, H 3.24, N 0.94%. Calculated for $[S_4Cd_{17}(SPh)_{28}](Me_4N)_2$: C 40.31, H 3.15, N 0.53%.

Heat-Treated $[E_4M_{10}(SPh)_{16}](Me_4N)_4$ (M = Cd, Zn; E = S, Se). Following the literature procedure,[19,30] $[S_4Cd_{10}(SPh)_{16}](Me_4N)_4$ was heat-treated at 300 °C under vacuum for 15 min. This yielded a pale yellow powder of $S_4Cd_{10}(SPh)_{12}$. The selenium cluster $[Se_4Cd_{10}(SPh)_{16}](Me_4N)_4$ and the zinc analogues $[S_4Zn_{10}(SPh)_{16}](Me_4N)_4$ and $[Se_4Zn_{10}(SPh)_{16}](Me_4N)_4$ were heat-treated in the same way, yielding respectively yellow and white powders. Elemental analyses: Found for heat-treated $[S_4Cd_{10}(SPh)_{16}](Me_4N)_4$: C 33.70, H 2.02, N 0.27%; C 37.85, H 2.89, N 0.96% (after recrystallization from pyridine/DMF). Calculated for $S_4Cd_{10}(SPh)_{12}$: C 33.75, H 2.36, N 0%. Found for heat-treated $[Se_4Cd_{10}(SPh)_{16}](Me_4N)_4$: C 31.71, H 2.02, N 0%. Calculated for $Se_4Cd_{10}(SPh)_{12}$: C 33.12, H 2.20, N 0%. In separate experiments, stoichiometric amounts of $(Me_4N)I$ and HSPh were added to $S_4Cd_{10}(SPh)_{12}$ dissolved in pyridine. This resulted in the conversion of the material to respectively $[S_4Cd_{10}(SPh)_{12}I_4]^{4-}$ and $[S_4Cd_{10}(SPh)_{16}]^{4-}$, as determined from the far-IR spectra.

$Cd_xS_y(SPh)_z$. A series of capped clusters with diameters ranging from ca. 10 to 40 Å were prepared using the literature method,[17] by mixing a solution of Cd^{2+} ions in acetonitrile with an acetonitrile solution of $S^{2-}$and PhSH in different ratios such that $2[Cd^{2+}] = [S^{2-}] + [PhSH]$. The powdery precipitates which were obtained for $[S^{2-}]/[PhSH]$ ratios of $^1/_3$, $^1/_2$, $^3/_4$, 2, and 5 ranged in color from pale yellow to light orange and were filtered and washed with methanol. The cluster sizes were estimated to be ca. 10, 15, 20, 30, and 40 Å with an estimated size dispersion of ∼20%, from the UV−visible spectra taken from these materials dissolved in acetonitrile. The empirical correlation given in the literature between the absorption maximum, corresponding to the excitation energy, and cluster size was used.[6] The excitation wavelength was determined by locating the peak in the second derivative of the absorption band. The values were 360, 380, 400, 430, and 450 nm, respectively.

Results and Discussion

Vibrational Modes of the SPh^- Surface Caps and of the CdE Core (E = S, Se) of $[E_4Cd_{10}(SPh)_{16}]^{4-}$. Before attempting to analyze the vibrational spectra of SPh^--capped nanoclusters of CdS, it is necessary to review the vibrational spectra of the corresponding bulk material. Cadmium sulfide can exist in two crystal phases: the low-temperature hexagonal (wurtzite) structure and the high-temperature cubic (sphalerite) phase. A wurtzite type crystal has C_{6v} symmetry with 4 atoms/unit cell. Group theory predicts 12 phonon branches, 9 optical and 3 acoustic. Of the 9 optical branches there

(20) Lee, G. S. H.; Fisher, K. J.; Craig, D. C.; Scudder, M. L.; Dance, I. G. *J. Am. Chem. Soc.* **1990**, *112*, 6435.
(21) Dance, I. G.; Choy, A.; Scudder, M. L. *J. Am. Chem. Soc.* **1984**, *106*, 6285.
(22) Lee, G. S. H.; Craig, D. C.; Ma, I.; Scudder M. L.; Bailey, T. D.; Dance, I. G. *J. Am. Chem. Soc.* **1988**, *110*, 4863.
(23) Vossmeyer, T.; Reck, G.; Katsikas, L.; Haupt, E. T. K.; Schulz, B.; Weller, H. *Science* **1995**, *267*, 1476.
(24) Nosaka, Y.; Shigeno, H.; Ikeuchi, T. *J. Phys. Chem.* **1995**, *99*, 8317.
(25) Shiang, J. J.; Risbud, S. H.; Alivisatos, A. P. *J. Chem. Phys.* **1993**, *98*, 8432.
(26) Shiang J. J.; Kadavanich, A. V.; Grubbs, R. K.; Alivisatos, A. P. *J. Phys Chem.* **1995**, *88*, 17417.
(27) Dean, P. A. W.; Vittal, J. J.; Payne, N. C. *Inorg. Chem.* **1987**, *26*, 1683.
(28) Dance, I. G.; Garbutt, R. G.; Craig, D. C.; Scudder, M. L. *Inorg. Chem.* **1987**, *26*, 4057.
(29) Lee, G. S. H. Ph.D. Thesis, University of New South Wales, Australia, 1993.
(30) Farneth, W. E.; Herron, N.; Wang, Y. *Chem. Mater.* **1992**, *4*, 916.

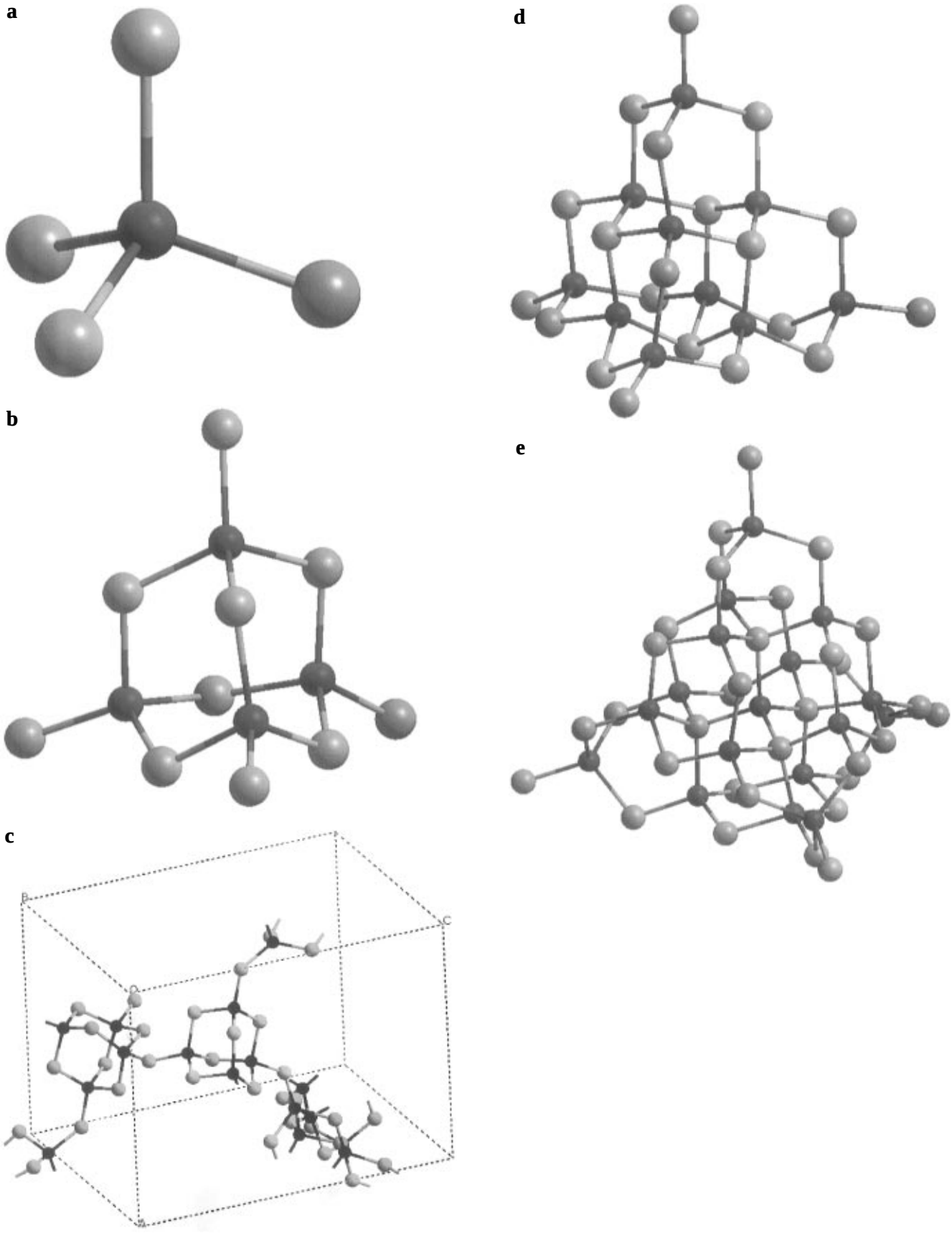

Figure 1. Structures of (a) $[Cd(SPh)_4]^{2-}$, (b) $[Cd_4(SPh)_{10}]^{2-}$, (c) $Cd(SPh)_2$, (d) $[S_4Cd_{10}(SPh)_{16}]^{4-}$, and (e) $[S_4Cd_{17}(SPh)_{28}]^{2-}$. The phenyl groups of the SPh^- ligands have been omitted for clarity. The structures were drawn with the Cerius[2] program using crystal structure data from the Cambridge database.

is one A_1 and one doubly degenerate E_1 which are both Raman and infrared active, two doubly degenerate E_2 branches which are Raman active only, and two inactive B_1 branches. For the infrared-active modes, the macroscopic electric field associated with the longitudinal phonons produces an additional stiffening and thereby

Table 1. Internal Modes and Corresponding Frequencies for Wurtzite CdS from Previous Raman and Infrared Work[31]

internal modes	Raman (cm^{-1})	IR (cm^{-1})
E_1 (transverse)	235	242
A_1 (transverse)	228	234
E_1 (longitudinal)	305	
A_1 (longitudinal)	305	305

lifts the degeneracy of the transverse and longitudinal modes.[31] The E_1 and A_1 longitudinal and transverse modes have previously been assigned to the frequencies given in Table 1.

A CdS cluster with surface-capping SPh^- ligands will have two different categories of vibrational modes: those involving the Cd−S bonds of the core and those of the Cd−SPh bonds of the surface. On the basis of a previous vibrational study of $Cd(SBu^t)_2$ and $Cd(SEt)_2$,[32] the frequencies of the (Cd−SPh) vibrations were also expected to occur in the low-frequency region. To assign the (Cd−SPh) frequencies and distinguish these bands from the Cd−S core frequencies, the spectra of the cadmium thiophenolate compounds $[Cd(SPh)_4](Me_4N)_2$, $[Cd_4(SPh)_{10}](Me_4N)_2$, and $Cd(SPh)_2$ were recorded. As seen in Figure 1 the structures of these compounds consist of structural elements that also constitute the cadmium thiophenolate surface of the clusters $[S_4Cd_{10}(SPh)_{16}](Me_4N)_4$ and $[S_4Cd_{17}(SPh)_{28}](Me_4N)_2$. Thus, additional bands in the spectra of these clusters would be due to the vibrations of the Cd−S bonds of the S_4Cd_6 and S_4Cd_{13} cluster cores.

The far-infrared spectra of $[Cd(SPh)_4](Me_4N)_2$, $[Cd_4(SPh)_{10}](Me_4N)_2$, and $Cd(SPh)_2$ are shown in Figure 2. The assignments of both IR and Raman bands are summarized in Table 2. The complex $[Cd(SPh)_4](Me_4N)_2$ has the simplest structure and contains $[Cd(SPh)_4]^{2-}$ tetrahedra with CdS_4 coordination, and with all the thiophenolate ions terminally bonded to Cd^{2+}. A C_2 symmetry was found for the $M(SC)_4$ core of the $[Cd(SPh)_4]^{2-}$ ion by Ueyama et al.[33] In the low-frequency region a band at 180 cm^{-1} (IR, R) was assigned to the $\nu(Cd-SPh^t)$ stretching vibrations (SPh^t denotes terminal SPh^- ligand). A higher frequency band at 338/339 cm^{-1} (IR/R) was assigned to a mode with both $\nu(Cd-SPh) + \delta(Cd-S-Ph)$ character. Our vibrational analysis agrees with these results. The predicted symmetry types and activities for the fundamentals of the CdS_4 core with C_2 point group are 4A(IR, R) + 5B(IR, R). These involve contributions from $Cd-SPh^t$ bond stretching $\nu(Cd-SPh^t)$ (2A + 2B) and bending vibrations $\delta(S-Cd-S)$ (2A + 3B). The strong infrared band with maximum at 178 cm^{-1} and shoulders at 162, 187, and 201 cm^{-1} seems to be in the correct position to be assigned to the four $\nu(Cd-SPh^t)$ stretching modes. The $\nu(Cd-SPh^t) + \delta(Cd-S-C)$ vibrations, expected at higher energies than the $\nu(Cd-SPh^t)$ stretches, can then be assigned to the band at 338 cm^{-1}. The two bands at 417 and 477 cm^{-1} which are present in the spectra of each of $[Cd(SPh)_4](Me_4N)_2$, $[Cd_4(SPh)_{10}](Me_4N)_2$, and $Cd(SPh)_2$ show little sensitivity to the different structures. This suggests that they do not involve (Cd−SPh) bonds but are due to the SPh^- ligand. In accord with the assignments made by Scott[34] for thiophenol (HSPh) and Whiffen[35] for chlorobenzene (ClPh; SH and Cl have similar relative molar masses, 33.07 and 35.45), we have assigned the 417 cm^{-1} frequency to the $\nu(C-S)$ stretching mode with A_1 symmetry (local C_{2v} symmetry group) and the 477 cm^{-1} band to the y-bending mode with B_1 symmetry.

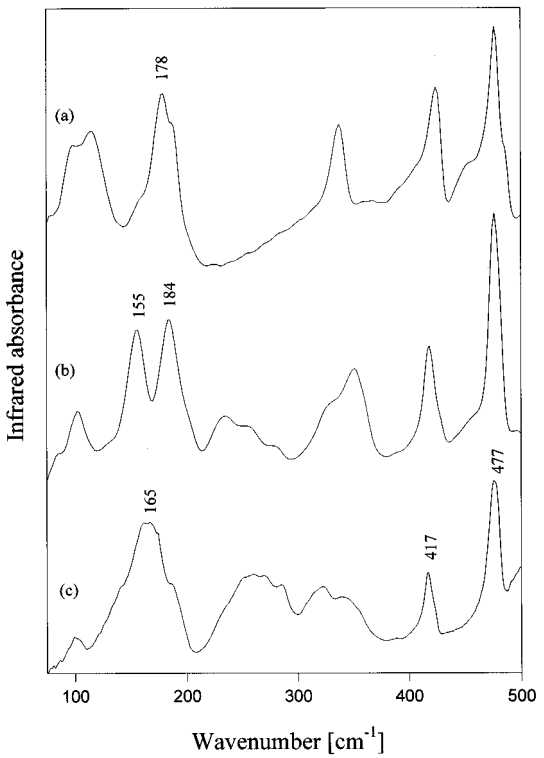

Figure 2. Low-frequency FT-IR spectra of (a) $[Cd(SPh)_4](Me_4N)_2$, (b) $[Cd_4(SPh)_{10}](Me_4N)_2$, and (c) $Cd(SPh)_2$.

The admantanoid cage $[Cd_4(SPh)_{10}]^{2-}$ [36] consists of four fused $Cd(SPh)_4$ tetrahedra with four terminal and six doubly bridging thiophenolate ligands. It possesses the molecular structure of octahedro-$(SPh)_6$-tetrahedro-$(MSPh)_4$ in which the M_4S_{10} core is structurally equivalent to a unit cell of the cubic (sphalerite) cadmium sulfide lattice. The structure also represents one of the four fused admantanoid cages that comprise the cluster $[S_4Cd_{10}(SPh)_{16}]^{4-}$.[21] The predicted symmetry types and activities of the stretching fundamentals of the Cd_4S_{10} core which has T_d symmetry are $A_1(R)$ and T_2 (IR, R) for the four terminal ligands and $A_1(R) + E(R) + T_1(R) + 2T_2$(IR, R) for the six bridging ligands. The $\nu(Cd-SPh^t)$ band of the terminal ligands in $[Cd_4(SPh)_{10}]^{2-}$ was expected at a slightly higher frequency than 178 cm^{-1} observed for $[Cd(SPh)_4]^{2-}$ on the basis that the mean $(Cd-SPh^t)$ bond length of 2.467 Å[36] is shorter compared with 2.541 Å[33] in $[Cd(SPh)_4]^{2-}$. The band at 184 cm^{-1} is therefore assigned to the $\nu(Cd-SPh^t)$ stretching frequency. Stretching vibrations of bridging ligands normally occur at a lower frequency than the terminal stretches. The mean bond length of the bridging ligands of 2.56 Å[36] is significantly longer than that for the four

(31) Tell, B.; Damen, T. C.; Porto, S. P. S. *Phys. Rev.* **1966**, *144*, 771.
(32) Canty, A. J.; Kishimoto, R.; Deacon, G. B.; Farquharson, G. J. *Inorg. Chim. Acta* **1976**, *20*, 161.
(33) Ueyama, N.; Sugawara, T.; Sasaki, K.; Nakamura, A.; Yamashita, S.; Wakatsuki, Y.; Yamazaki, H.; Yasuoka, N. *Inorg. Chem.* **1988**, *27*, 741.
(34) Scott, D. W.; McCullough J. P.; Hubbard, W. N.; Messerly, J. F.; Hossenlop, I. A.; Frow, F. R.; Waddington, G. *J. Am. Chem. Soc.* **1956**, *5*, 5463.
(35) Whiffen, D. H. *J. Chem. Soc.* **1956**, 1350.
(36) Hagen K. S.; Holm, R. S. *Inorg. Chem.* **1983**, *22*, 3171.

Table 2. Assignments of Bands in the Low-Frequency (50−500 cm^{-1}) Infrared and Raman Spectra of $[Cd(SPh)_4](Me_4N)_2$, $[Cd_4(SPh)_{10}](Me_4N)_2$, $Cd(SPh)_2$, $[S_4Cd_{10}(SPh)_{16}](Me_4N)_4$, and $[Se_4Cd_{10}(SPh)_{16}](Me_4N)_4$[a]

	$Cd(SPh)_2$		$[Cd(SPh)_4]^{2-}$		$[Cd_4(SPh)_{10}]^{2-}$		$[S_4Cd_{10}(SPh)_{16}]^{4-}$		$[Se_4Cd_{10}(SPh)_{16}]^{4-}$	
assignment	IR	Raman	IR	Raman	IR	Raman	IR	Raman	IR	Raman
$\delta(SPh^-)$	57w	42m	57w		56w	56w	55w	51wsh		50w
	86w	94m	78wsh	79w	86wsh		77wsh	91s	87w	81m
	100w		100m		102w		100wsh	101wsh	97w	98wsh
			115m	109m						
$\nu(Cd-SPh^t)$			162wsh							
			178s	178s	184s	188m	169s	187m	170s	173w
			187ssh							
			201wsh	202m						
$\nu(Cd-SPh^b)$	141wsh	142s								
	164s	169s			155s	156s	150s	160s	148s	151s
	185msh	192w			184s	188m	169s	187m	170s	173m
$\nu(Cd-Se)$									204s	206w
$\delta(Cd-S_b-C)$	259m	251mb			235w	235m	237wsh	246sb	235m	249mb
	270m	266−335w			253w		246m		245m	
	286m				279w		334w		257m	
	321m				336m	328w		315m	318m	313wb
	341m									
$\nu(Cd-S)$							288s	292w		
$\delta(Cd-S_t-C)$			338m	341m	350m	352 w	334w	338w	339m	313wb
$\nu(C-S)$	417s	422m	424s	428m	418s	422m	418m	423s	417s	421m
$\delta(SPh^-)$ (y)	477s	481w	477s	479w	476s	479w	478s	482w	478w	479w

[a] Intensities: s = strong, m = medium, w = weak, b = broad, sh = shoulder, S^t and SPh^t = terminal SPh^-, S^b and SPh^b = doubly bridging SPh^-.

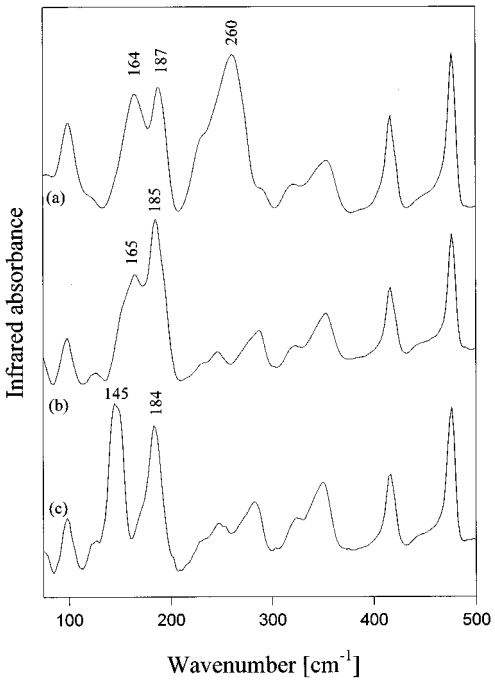

Figure 3. Low-frequency FT-IR spectra of (a) $[Cd_4Cl_4(SPh)_6](Et_4N)_2$, (b) $[Cd_4Br_4(SPh)_6](Et_4N)_2$, and (c) $[Cd_4I_4(SPh)_6](Et_4N)_2$.

terminal ligands (2.467 Å). The second strong band at 155 cm^{-1} therefore matches the expected position for the $\nu(Cd-SPh^b)$ stretching frequencies. To test if one of the two T_2 modes of the bridging SPh^- ligands is contributing to the strong intensity of the 184 cm^{-1} band assigned to the $\nu(Cd-SPh^t)$ stretching frequency, we recorded the spectra of the three structural analogues $[Cd_4X_4(SPh)_6]^{2-}$ (X = Cl, Br, I) in which the four terminal SPh^- ligands have been replaced by a halide. The frequency of the $\nu(Cd-X)$ stretches of the terminal halide ligands was expected to depend on the halide type. The spectra are shown in Figure 3. For X = Cl a strong band is observed at 260 cm^{-1} which can be assigned to the $\nu(Cd-Cl)$ stretches. The higher frequency position compared with 184 cm^{-1} for SPh^- is consistent with the smaller relative molar mass of 32.06 for Cl^- compared with 109.17 for SPh^-. Two distinct frequencies are still observed at 187 and 164 cm^{-1} consistent with the two T_2 $\nu(Cd-S_b)$ stretching modes of the bridging SPh^- ligands. The $\nu(Cd-X)$ stretching frequency moves downward to 185 cm^{-1} for the heavier Br^- ligand and superimposes the higher of the two $\nu(Cd-S_b)$ bands. With X = I a further downward shift of the $\nu(Cd-X)$ band to 145 cm^{-1} is observed. In this case the lower of the two $\nu(Cd-SPh^b)$ bands become masked by the $\nu(Cd-I)$ band. In the corresponding Raman spectra (not shown) the $\nu(Cd-X)$ bands appeared as less intense peaks. The two $\nu(Cd-SPh^b)$ frequencies appeared as one very strong band at about 151 cm^{-1} and a weaker band at about 182 cm^{-1}, in accord with the Raman spectrum of $[Cd_4(SPh)_{10}](Me_4N)_2$ (refer to Table 2). One can conclude that the $\nu(Cd-SPh^t)$ stretching frequency of the terminal SPh^- ligands and one of the two T_2 $\nu(Cd-SPh^b)$ stretching frequencies of the bridging ligands in $[Cd_4(SPh)_{10}](Me_4N)_2$ both occur around 185 cm^{-1}. The second $\nu(Cd-SPh^b)$ band occurs in the 155 cm^{-1} region. The above assignments are further supported by the spectrum of $Cd(SPh)_2$ shown in Figure 2c. This structure has only bridging SPh^- ligands and consists of admantanoid cages comprised of four Cd atoms and six doubly bridging SPh^- ligands connected in three dimensions by four doubly bridging SPh^- ligands.[29] A strong $\nu(Cd-SPh^b)$ band with several shoulders is observed at 165 cm^{-1}. The slightly higher frequency than 155 cm^{-1} observed for $[Cd_4(SPh)_{10}]^{2-}$ is in accord with the slightly shorter mean (Cd−SPh) bond lengths of the six intracage (2.543 Å) and of the four intercage ligands (2.530 Å)[28] compared with 2.56 Å for $[Cd_4(SPh)_{10}]^{2-}$. Also, the larger bandwidth in this spectrum can be explained by the difference in the bond lengths between the two types of bridging SPh^- ligands. The $\delta(Cd-S_b-C)$ bending vibrations are assigned to bands in the regions 235−270 and 315−350 cm^{-1} on the basis that these bands are present in the structures $[Cd_4(SPh)_{10}]^{2-}$, $Cd(SPh)_2$, $[S_4Cd_{10}(SPh)_{16}]^{4-}$, $[Se_4Cd_{10}(SPh)_{16}]^{4-}$, and $[S_4Cd_{17}$-

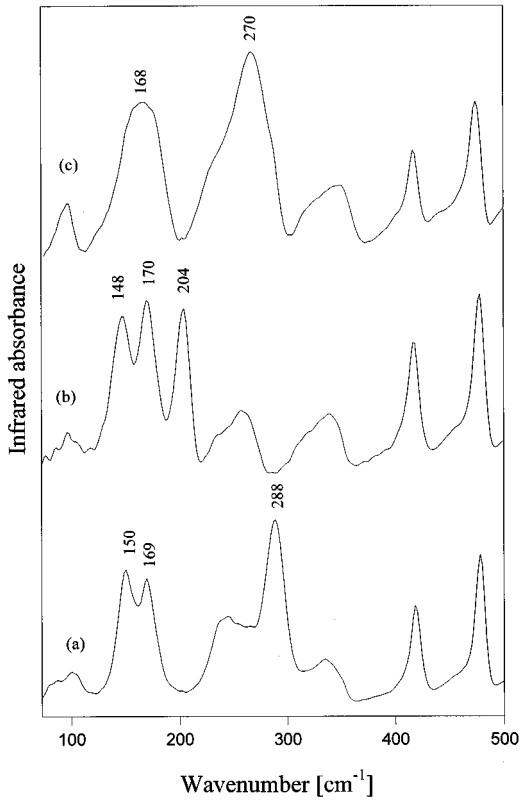

Figure 4. Low-frequency FT-IR spectra of (a) $[S_4Cd_{10}(SPh)_{16}](Me_4N)_4$, (b) $[Se_4Cd_{10}(SPh)_{16}](Me_4N)_4$, and (c) $[S_4Cd_{17}(SPh)_{28}](Me_4N)_2$. The ν(Cd−S) and ν(Cd−Se) stretching frequencies of the internal (Cd−S) and (Cd−Se) bonds of the cluster cores of $[S_4Cd_{10}(SPh)_{16}]^{4-}$ and $[Se_4Cd_{10}(SPh)_{16}]^{4-}$ occur at (a) 288 cm^{-1} and (b) 204 cm^{-1}. The corresponding ν(Cd−S) stretching frequencies of the tetracoordinated sulfurs in the core of $[S_4Cd_{17}(SPh)_{28}]^{2-}$ occur at (c) 270 cm^{-1}. Refer also to the structures in Figure 1d,e. The ν(Cd−SPh) stretching frequencies of the terminal and bridging SPh^- ligands occur at (a) 150, 169, (b) 148, 170, and (c) 168 cm^{-1}.

$(SPh)_{28}]^{2-}$ (see below) all of which have bridging ligands, but absent in $[Cd(SPh)_4](Me_4N)_2$ which only have terminal ligands.

We now turn to the vibrational spectrum of the CdS cluster $[S_4Cd_{10}(SPh)_{16}](Me_4N)_4$. The $[S_4Cd_{10}(SPh)_{16}]^{4-}$ ion shown in Figure 1d is a supertetrahedral fragment of the cubic (sphalerite) CdS lattice terminated by bridging and terminal thiophenolate ligands.[21] The cluster has virtual T_d symmetry for the $Cd_{10}S_{20}$ core which consists of six inner Cd atoms bridged by four triply bridging sulfide ions, four outer cadmium atoms each connected by three doubly bridging thiophenolate ligands, and four outer terminal thiophenolate ligands. The diameter of the S_4Cd_{10} core is ca. 7 Å. The far-infrared spectrum shown in Figure 4a is very similar to that of $[Cd_4(SPh)_{10}](Me_4N)_2$. This is consistent with the adamantane basis of both structure types. The ν(Cd−SPh^t) and ν(Cd−SPh^b) bands in $[S_4Cd_{10}(SPh)_{16}]^{4-}$ appear at 169 and 150 cm^{-1}. One additional strong feature is observed at 288 cm^{-1}. This band is near the 242 cm^{-1} peak position of the transverse E_1 mode of bulk (wurtzite) CdS, and we have assigned it to the ν(Cd−S) stretching frequencies of the (Cd−S) bonds of the S_4Cd_6 core. For the isostructural selenide cluster $[Se_4Cd_{10}(SPh)_{16}](Me_4N)_4$ the corresponding ν(Cd−Se) band occurs at 204 cm^{-1} (Figure 4b). This downward shift by 84 cm^{-1} is consistent with the larger mass of the selenium atom. The Raman spectra of $[S_4Cd_{10}(SPh)_{16}]$-

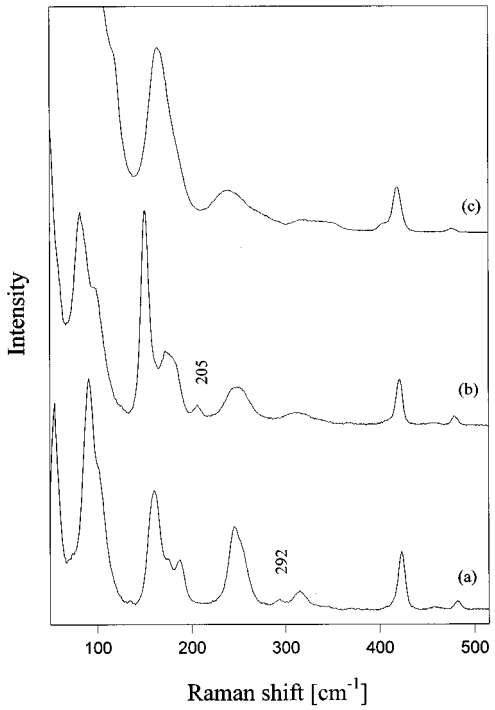

Figure 5. Low-frequency Raman spectra of (a) $[S_4Cd_{10}(SPh)_{16}](Me_4N)_4$, (b) $[Se_4Cd_{10}(SPh)_{16}](Me_4N)_4$, and (c) $[S_4Cd_{17}(SPh)_{28}](Me_4N)_2$. The ν(Cd−S) and ν(Cd−Se) stretching frequencies of the internal Cd−S and Cd−Se bonds of the cluster cores of $[S_4Cd_{10}(SPh)_{16}]^{4-}$, $[Se_4Cd_{10}(SPh)_{16}]^{4-}$, and $[S_4Cd_{17}(SPh)_{28}]^{2-}$ occur as very weak bands at (a) 292, (b) 205, and (c) 270 cm^{-1}. The strong bands in the 150−200 cm^{-1} region in each spectrum are due to the ν(Cd−SPh) stretching frequencies of the terminal and bridging SPh^- ligands.

$(Me_4N)_4$ and $[Se_4Cd_{10}(SPh)_{16}](Me_4N)_4$ shown in Figure 5a,b are also nearly identical except for two weak bands at 292 and 206 cm^{-1}. These correspond to the ν(Cd−S) and the ν(Cd−Se) stretching frequencies at 288 and 205 cm^{-1} in the respective infrared spectra. The very low intensities of these frequencies in the Raman spectrum probably explains why Dance[21] in the original report of this cluster, which did not include the far-IR spectrum, was not able to distinguish the bands involving the Cd−S bonds of the core from those of the Cd−SPh bonds of the surface. There are two interesting features to be noted about the spectra of these clusters. While the ν(Cd−E) core band shows a strong shift for S and Se, the rest of the spectrum remains essentially unchanged. This suggests that the vibrational modes of the Cd−E bonds are not coupled with those of the Cd−SPh bonds of the six bridging SPh^- ligands which are also connected to the inner cadmium atoms. Further evidence for this is the close similarity in the spectra of $[Cd_4(SPh)_{10}](Me_4N)_2$ and $[S_4Cd_{10}(SPh)_{16}](Me_4N)_4$. The two spectra look identical except for the additional ν(Cd−S) core band in $[S_4Cd_{10}(SPh)_{16}](Me_4N)_4$. Vibrational analysis of the S_4Cd_6 core with T_d point group predicts a total of 24 vibrational modes: $2A_1 + 2E + 2T_1 + 4T_2$, where the E modes are doubly degenerate and the T_1 and T_2 modes are triply degenerate. The 12 stretching modes are $A_1(R) + E(R) + T_1 + 2T_2$ (IR, R); thus, four frequencies are expected in the Raman spectrum and two in the infrared spectrum. It is noteworthy that the ν(Cd−E) frequencies give only a single and relatively narrow band in both the infrared and the Raman spectrum. This shows that all the

predicted stretching modes occur at very similar frequencies.

The ν(Cd−S) Frequencies in Clusters with Increasing Core Diameter from 9 to ~40 Å. Having identified for the $[S_4Cd_{10}(SPh)_{16}]^{4-}$ cluster the ν(Cd−S) stretching frequencies of the core and the ν(Cd−SPh^t) and ν(Cd−SPh^b) stretching frequencies of the terminal and bridging thiophenolate capping ligands, our aim was to investigate the spectra of clusters with increasing CdS core diameter. The 9 Å cluster ion $[S_4Cd_{17}(SPh)_{28}]^{2-}$ of $[S_4Cd_{17}(SPh)_{28}](Me_4N)_2$[22] has a core with tetracoordinated sulfides as in bulk CdS (Figure 1e). Each of the four quadruply bridging S^{2-} ions is connected to a central cadmium atom, Cd^i, and three cadmium atoms, Cd^c, each with tetrahedral (μ_4-S)(μ-SPh)$_2$(SPh) coordination and which are part of a cuboctahedron. At the corners of the cluster are four cadmium atoms each with tetrahedral (μ-SPh)$_3$−(μ-SPh) coordination. The far-infrared spectrum shown in Figure 4c shows a strong ν(Cd−S) core band at 270 cm^{-1}. Compared with $[S_4Cd_{10}(SPh)_{16}]^{4-}$, whose core has only triply bridging sulfides, the ν(Cd−S) frequency is shifted downward by 18 cm^{-1}. This agrees with the longer (Cd−S) bond distances of 2.497 Å (Cd^i−S) and 2.53 Å (Cd^c−S) in $[S_4Cd_{17}(SPh)_{28}]^{2-}$ compared with 2.484 Å in $[S_4Cd_{10}(SPh)_{16}]^{4-}$. The lower frequency region shows a broad band at 168 cm^{-1} in the infrared spectrum and at 164 cm^{-1} in the Raman spectrum (Figure 5c). These bands occur in the region assigned to the ν(Cd−SPh^b) stretching frequencies of the bridging ligands in $[S_4Cd_{10}(SPh)_{16}]^{4-}$ (169, 150/187, 160 cm^{-1} (IR/R), and this is consistent with the similar (Cd−S$_b$) bond lengths of 2.53 Å in $[S_4Cd_{17}(SPh)_{28}]^{2-}$ and 2.59 Å in $[S_4Cd_{10}(SPh)_{16}]^{4-}$. Any contribution from the ν(Cd−SPh^t) stretching frequency of the terminal SPh$^-$ ligands in $[S_4Cd_{17}(SPh)_{28}]^{2-}$ is expected to be very small as only 4 of the 28 ligands are terminal. As for $[S_4Cd_{10}(SPh)_{16}]^{4-}$, the ν(Cd−S) core band in the Raman spectrum of $[S_4Cd_{17}(SPh)_{28}]^{2-}$ is very weak and appears to be masked by bands due to the δ(Cd−S$_b$−C) bending modes in the same region.

We now study a series of clusters with diameters ranging from ca. 10 to 40 Å. These materials were prepared by mixing solutions of Cd^{2+} with solutions of S^{2-} and PhSH in different ratios. Figure 6 shows the far-infrared spectra of these clusters and of bulk (wurtzite) CdS. As the sulfur-to-thiophenolate ratio increases, yielding a material with increasing CdS core size, the ν(Cd−S) core band in the region 240−290 cm^{-1} becomes progressively more intense and broad. Corresponding to the increased intensity and width of the ν(Cd−S) core band is a decrease in the intensity of the ν(Cd−SPh^b) stretching frequencies of the bridging SPh$^-$ ligands at ca. 160 cm^{-1} and in the two thiophenolate bands at 417 and 478 cm^{-1}. This decrease in intensity is in agreement with the decrease in the overall proportion of thiophenolate as the proportion of sulfide is increased. The increasing ν(Cd−S) bandwidth is consistent with the increasing number of vibrations associated with the growing CdS core. The size dispersion in these materials is estimated to ca. 20% from the UV−visible absorption data and the X-ray data by Herron et al.[17] This is expected to contribute to the bandwidth. The peak position of the ν(Cd−S) core band shifts downward toward the band maximum of 241 cm^{-1} for bulk CdS. The downward shift in the ν(Cd−S) stretching frequencies with increased cluster size can be explained by a progressive increase in the average Cd−S bond length. The Cd−S bond lengths and the corresponding ν(Cd−S) core band maxima for $[S_4Cd_{10}(SPh)_{16}]^{4-}$, $[S_4Cd_{17}(SPh)_{28}]^{2-}$, and bulk wurtzite CdS are 2.484 Å/288 cm^{-1}, 2.497 Å/270 cm^{-1}, and 2.519 Å/242 cm^{-1}. The mean value of these shifts is 1273 cm^{-1} Å^{-1}. In Figure 7 the ν(Cd−S) core band maxima for $[S_4Cd_{10}(SPh)_{16}]^{4-}$ and $[S_4Cd_{17}(SPh)_{28}]^{2-}$ and for the materials in Figure 6 are plotted versus cluster diameters. The plot shows that an indication of the cluster diameter can be obtained from the peak position of the far-IR ν(Cd−S) core band. The error of such an estimate is ca. ±2 Å.

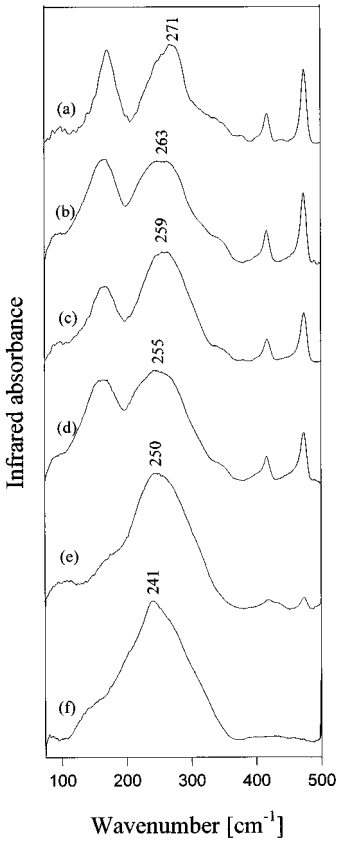

Figure 6. Low-frequency FT-IR spectra of SPh-capped CdS clusters of increasing core diameters from 10 to 40 Å and of bulk CdS: (a) 10, (b) 15, (c) 20, (d) 30, (e) 40 Å, and (f) bulk (wurtzite) CdS. The spectra show a progressive broadening and shift of the ν(Cd−S) core band with increasing cluster size. The ν(Cd−S) stretching frequency of the TO (E_1 mode) of bulk CdS is at 241 cm^{-1}. The downward shift in frequency is consistent with an increase in the average (Cd−S) bond length with increasing cluster size (see text).

Resonance Raman spectra of these materials showed one mode at ca. 305 cm^{-1} and its first overtone at 610 cm^{-1}. Background fluorescence resulted in poor spectra, particularly for the smallest clusters. We were therefore unable to investigate the effects of cluster size on peak positions and peak-widths in the Raman spectra. Spectra which are not obscured by fluorescence should be obtainable with the use of a nonresonating light source such as the 1064 nm Nd:YAG laser commonly used with FT-Raman spectrometers.

$[S_4Cd_{10}(SPh)_{12}]$. The sensitivity of the far-IR ν(Cd−S) core band to changes in core structure and cluster size provides a method for characterizing CdS cluster

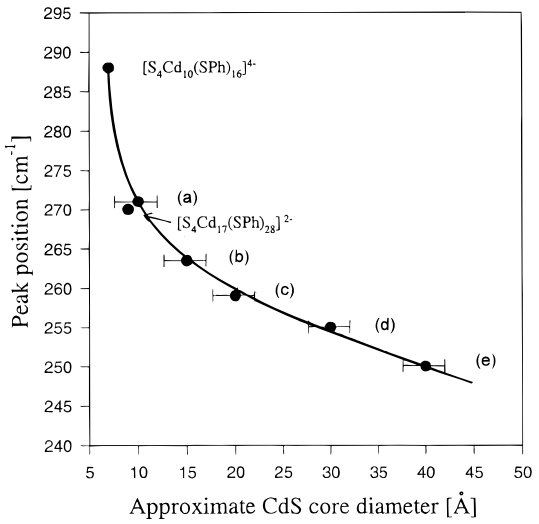

Figure 7. Plot of FT-IR peak position of the ν(Cd−S) core band versus particle diameter for CdS clusters. The cluster materials (a−e) correspond to the materials in Figure 6 a−e.

materials. We attempted the synthesis of the 15 Å cluster $[S_{14}Cd_{32}(SPh)_{36}]\cdot 4DMF$ reported by Herron et al.[19] The cluster $[S_4Cd_{10}(SPh)_{16}](Me_4N)_4$ was heated under vacuum at 10 °C/min to 300 °C and held there for 15 min. This produced a pale yellow powder. Combined TGA and mass spectroscopy data obtained by Farneth et al.[30] showed that the heating of $[S_4Cd_{10}(SPh)_{16}](Me_4N)_4$ results in a loss of four $(Me_4N)SPh$ per cluster, leaving a material with the composition $S_4Cd_{10}(SPh)_{12}$. Our STA analysis showed a weight loss of 25.0%, which agrees reasonably well with the calculated value of 22.2%. The elemental analysis was also found to agree with $S_4Cd_{10}(SPh)_{12}$. Recrystallization from pyridine containing DMF was reported to yield yellow cubic crystals of $[S_{14}Cd_{32}(SPh)_{36}]\cdot 4DMF$. Unfortunately, this was not successful in our hands. However, we are able to analyze the vibrational spectrum of the $S_4Cd_{10}(SPh)_{12}$ intermediate and discuss the possible structures of this compound. This is obviously relevant to the mechanism of formation of the $[S_{14}Cd_{32}(SPh)_{36}]\cdot 4DMF$ cluster. The infrared spectrum of $S_4Cd_{10}(SPh)_{12}$ in Figure 8a shows a strong ν(Cd−S) core band at 265 cm^{-1}. The intensity of the ν(Cd−S) core band relative to the thiophenolate bands at 417 and 477 cm^{-1} has decreased compared with the spectrum of $[S_4Cd_{10}(SPh)_{16}](Me_4N)_4$. This is consistent with the decrease in the ratio of thiophenolate to CdS in this material. Farneth suggested that the four SPh^- ligands lost during heating are most probably the terminal ligands. Consistent with this is the observation of only one band at 170/167 cm^{-1} (IR/R) in the frequency region assigned to the ν(Cd−SPh^t) and ν(Cd−SPh^b) stretching frequencies. However, since the ν(Cd−SPh^t) and ν(Cd−SPh^b) stretching frequencies have been shown to overlap in this region in the spectra of $[Cd_4(SPh)_{10}](Me_4N)_2$ and $[S_4Cd_{10}(SPh)_{16}](Me_4N)_4$, the IR result is not conclusive. However, the removal of the four terminal SPh^- ligands from $[S_4Cd_{10}(SPh)_{16}]^{4-}$ would leave four Cd atoms uncoordinated (refer to Figure 1d). Two possible changes in bonding and structure in $S_4Cd_{10}(SPh)_{12}$ were suggested by Farneth. To retain the structural integrity of $[S_4Cd_{10}(SPh)_{16}]^{4-}$, the terminal Cd atoms can coordinate to the tricoordinate sulfur atoms on the faces of the pyramid, either inter- or intramolecularly, forming

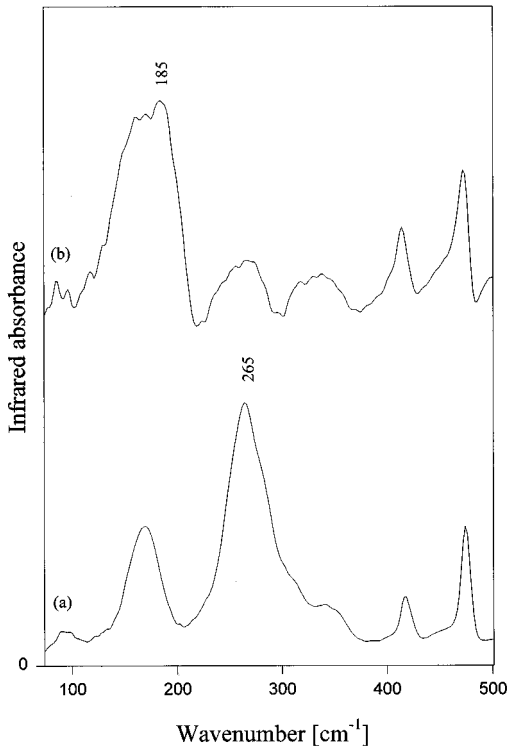

Figure 8. Low-frequency FT-IR spectra of (a) $[S_4Cd_{10}(SPh)_{12}]$ and (b) $[Se_4Cd_{10}(SPh)_{12}]$ formed by heating $[S_4Cd_{10}(SPh)_{16}](Me_4N)_4$ and $[Se_4Cd_{10}(SPh)_{16}](Me_4N)_4$ at 300 °C. The ν(Cd−S) and ν(Cd−Se) stretching frequencies of the internal (Cd−S) and (Cd−Se) bonds of the cluster cores have shifted (a) to 265 cm^{-1} from 288 cm^{-1} in $[S_4Cd_{10}(SPh)_{16}](Me_4N)_4$ and (b) to 185 cm^{-1} from 205 cm^{-1} in $[Se_4Cd_{10}(SPh)_{16}](Me_4N)_4$. These shifts to higher frequencies are interpreted in terms of a change in bonding from the triply bridging sulfur and selenium atoms of the cores in the starting materials to tetracoordination of these atoms in the cores of the heat-treated materials (see text).

a tetrahedral sulfur connected to four cadmium atoms. The 265 cm^{-1} position of the ν(Cd−S) core band in $S_4Cd_{10}(SPh)_{12}$ is close to that of 270 cm^{-1} observed for $[S_4Cd_{17}(SPh)_{28}]^{2-}$, and this suggests tetracoordinated sulfurs. An additional indication of this is a weak UV-absorption band at 350 nm for $S_4Cd_{10}(SPh)_{12}$. This absorption is not present in the starting material $[S_4Cd_{10}(SPh)_{16}]^{4-}$, which absorbs only below 300 nm.[37] It is known that the lowest optical absorption of either bulk CdS or CdS clusters corresponds mainly to the transfer of an electron from a tetrahedral sulfur (HOMO or valence band) to cadmium atoms (LUMO or conduction band).[18] The absorption band at 350 nm is close to that of 351 nm for the proposed 10 Å cluster $[S_{13}Cd_{22}(SPh)_{20}]^{8-}$,[18] which has one tetrahedral sulfur, and to that of 358 nm for the even larger 15 Å cluster $[S_{14}Cd_{32}(SPh)_{36}]\cdot 4DMF$.[19] Thus, from these absorption data one cannot discount the possibility that the material may consist of clusters with more than four sulfides in the core, i.e., a larger cluster species than the $[S_4Cd_{10}(SPh)_{16}](Me_4N)_4$ starting cluster. To test this, we added in separate experiments stoichiometric amounts of $(Me_4N)I$ or of HSPh and $(Me_4N)Cl$ to a solution of the $S_4Cd_{10}(SPh)_{12}$ compound in pyridine. This resulted in almost complete conversion of the $S_4Cd_{10}(SPh)_{12}$ material to $[S_4Cd_{10}(SPh)_{12}I_4]^{4-}$ or to $[S_4Cd_{10}(SPh)_{16}]^{4-}$,

(37) Türk, T.; Resh, U.; Fox, M. A.; Vogler, A. *J. Phys. Chem.* **1992**, *96*, 3818.

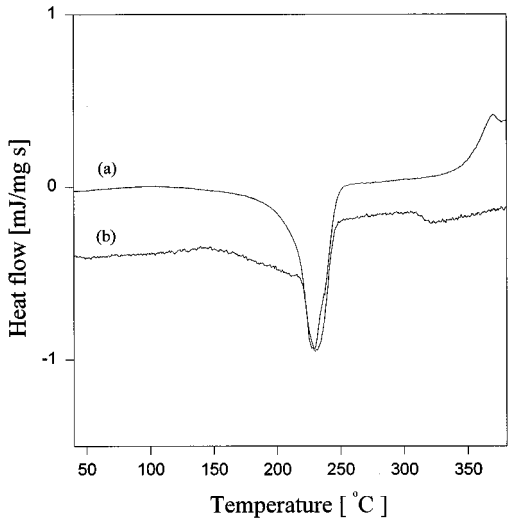

Figure 9. DSC thermal analysis traces (35−380 °C) of (a) $[S_4Cd_{10}(SPh)_{16}](Me_4N)_4$ and (b) $[Se_4Cd_{10}(SPh)_{16}](Me_4N)_4$. An exotherm at ca. 225 °C corresponds to the loss of four (Me_4N)-SPh units per cluster.

respectively. These results would seem likely only from a cluster material of structural integrity similar to that of the starting material. Addition of an excess of PhSH to CdS clusters is not known to "shrink" the clusters, so that cannot explain these reactions. In conclusion, the IR data give evidence of $S_4Cd_{10}(SPh)_{12}$ clusters with tetracoordinated sulfurs in the core. These are formed by the terminal Cd atoms which coordinate to the tricoordinate sulfur atoms on the faces of the pyramid either inter- or intramolecularly.

Thermal analysis (DSC) of $[S_4Cd_{10}(SPh)_{16}](Me_4N)_4$ and $[Se_4Cd_{10}(SPh)_{16}](Me_4N)_4$ show essentially identical traces (Figure 9a,b). The exotherm at about 225 °C corresponds to the temperature of the onset of loss of the four (Me_4N)SPh units. This exotherm was absent in the heat-treated materials. The similar decomposition of the selenide cluster $[Se_4Cd_{10}(SPh)_{16}](Me_4N)_4$ led us to heat-treat this material in the exact same manner. The ν(Cd−Se) core band of the yellow solid material that formed shifts to 185 cm^{-1} from 205 cm^{-1} in the starting material (Figure 8b). A 20 cm^{-1} downward shift was also observed for $S_4Cd_{10}(SPh)_{12}$. Other band features, including bandwidths and relative intensities, also match with the spectrum of $S_4Cd_{10}(SPh)_{12}$. The frequency region 220−350 cm^{-1} is not masked by the downshifted ν(Cd−Se) core band and shows the two characteristic band regions 230−290 and 310−350 cm^{-1} assigned to the $\delta(Cd-S_b-C)$ bending modes of the bridging ligands in the spectrum of $[S_4Cd_{10}(SPh)_{16}](Me_4N)_4$. On the basis of the identical thermal properties and the close matching with the spectrum of $S_4Cd_{10}(SPh)_{12}$, we conclude that the material is $Se_4Cd_{10}(SPh)_{12}$.

Conclusions

From the present work we can conclude that low-frequency FT-IR is a valuable method for characterizing thiophenolate-capped metal chalcogenide clusters. High sensitivity to the structure type and the identity of the metal−chalcogenide bond gives rise to spectra with well-resolved core bands and ligand bands. Far-infrared measurements have the advantages of being simple and quick to perform, thus making it an ideal technique for routine measurements. In the spectra of the clusters $[E_4Cd_{10}(SPh)_{16}](Me_4N)_4$ (E = S, Se) bands at 288 and 204 cm^{-1} are assigned to the ν(Cd−E) stretching modes of the internal Cd−E bonds of the cluster core. The ν(Cd−SPh) stretching frequencies of the bridging and terminal SPh^- ligands which cap the cluster core are assigned to bands in the region 150−187 cm^{-1}. The ν(Cd−S) core band for $[S_4Cd_{17}(SPh)_{28}](Me_4N)_2$ with tetracoordinated sulfides, as in bulk CdS, is observed at 270 cm^{-1}. The far-infrared ν(Cd−S) core band shows a progressive broadening and shift from 270 cm^{-1} toward the peak position of 241 cm^{-1} in bulk CdS with increasing cluster size up to ca. 40 Å. This shift is interpreted in terms of an increase in the average Cd−S bond length.

Raman spectroscopy of the SPh^--capped CdS clusters suffers from very weak intensities of the ν(Cd−S) stretching frequencies, and resonance Raman spectroscopy is limited by a strong fluorescence background.

Acknowledgment. We thank 3M for support of this work through financial support and a Ph.D. scholarship to T. Løver. We also thank the University of Auckland for financial support.

CM960534S